

ARCHI: a New Redundant Parallel Mechanism – Modeling, Control and First Results

Frederic Marquet, Sebastien Krut, Olivier Company and Francois Pierrot
LIRMM - UMR 5506 CNRS / UM2
161, rue Ada - 34392 Montpellier cedex 5, France
<marquet, krut, company, pierrot>@lirmm.fr

Abstract

This paper presents a 3-dof redundant parallel mechanism, ARCHI, designed as a sub-part of a 5-axis hybrid machine. The redundant parallel mechanism design and its models are recalled; different ways for its control and first motion results are presented, proving the ability of ARCHI to offer an unlimited rotation capability.

1. Introduction

After Gough [1] and Stewart [2] in the 50's and 60's introducing the idea of 'hexapods' (6-dof) [3][4], Clavel and his Delta structure [5] in the late 80's opened a new era with machines able to reach extremely high performances, used first for pick-and-place operations, and more recently for 3 or 5-axis machining. Considering the machining of complex shape objects, the solution often proposed by parallel mechanisms is dramatically different from the solution in use in industry. In fact, industrial machines are based on a 5-dof serial chain whose weak point is the 'head', *i.e.* the last two rotating joints; on the other hand, most parallel-mechanism-based machines rely on a 6-dof arrangement. Different designs have proven the efficiency of parallel mechanisms in this type of applications [6][7]. Approaches using less actuators (that is, five actuators for five machining axis) have been proposed recently, but they suffer from the same limitation than fully parallel chains: a limited tilting angle. Hybrid serial/parallel or parallel/serial structures (Tricept [8], Eclipse [9], DS Technologies Sprint) are solutions for 5-axis machining: the parallel/serial arrangement of Tricept offers a good dynamic behavior thanks to its parallel sub-part, but it still suffers from the limitations of a serial 'head'; Sprint architecture guarantees a good behavior of the 'head' but is limited in terms of tilting angle. In this paper, a solution based on the principle of Motion-Sharing where both the tool and the work-piece are moved, and where at least a part of the motion is due to parallel chains is studied. A new parallel redundant structure, ARCHI, has been designed as a part of a 5-axis equipment for machining. Its basic design and models are presented, and control strategies are discussed.

2. Motion-Sharing¹: ARCHI basic design

One possible design, based on the so-called H4 structures [10], where 4 dof are dedicated to the tool motion, and 1 dof

is at work-piece level has already been introduced. ARCHI is a solution giving the tool a complete planar motion (2 translations, 1 rotation), and letting the work-piece be moved along the remaining translation axis and about the remaining rotation axis. With ARCHI concept efforts are focused on planar parallel mechanisms. Such mechanisms have been intensively studied (see [11]) and it turns out it is not possible to obtain a large range of motion in rotation with classical arrangements. This is obviously because of the existence of singular positions, and among them, more specifically over-mobility singular positions where the machine stiffness is zero. The machine developed is designed to allow unlimited rotation capability thanks to a redundant parallel kinematics mechanism. Figure 1 includes the ARCHI 'arrangement graph' and a schematic view: four linear drives are fixed on the base, and then linked to the nacelle (carrying the spindle) thanks to R - R or U - S chains (P: Prismatic joint, U: Universal, S: Spherical, R: Revolute); on the work-piece side, two joints are arranged in a serial way. Two (parallel) arms are moving in a (x, y) plane and linked together *via* a rigid body and two revolute joints.

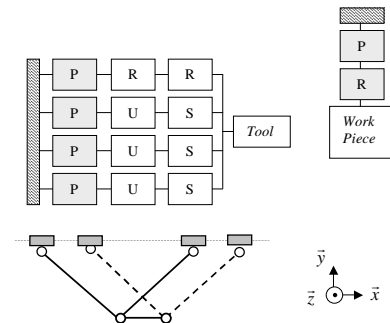


Figure 1. ARCHI basic design.

Indeed, when the nacelle rotates from 0 to 2π , each chain is in a 'singular' position when the 'leg' is aligned with the nacelle: the singular chain cannot produce any torque about \vec{z} axis (Figure 2). However, when a chain is singular, the three other chains are not, and the complete mechanical structure remains controllable. Such mechanisms offer in addition another advantage: they are extremely easy to build and assemble. The first ARCHI prototype is designed as a simple test-bed able to offer good performances: four LinearDrives motors, a FAEMAT spindle and few off-the-shelve components are used.

¹ This concept already exists for some 'serial' machine-tools, and has been called the 'left-hand/right-hand' paradigm in the robotics community.

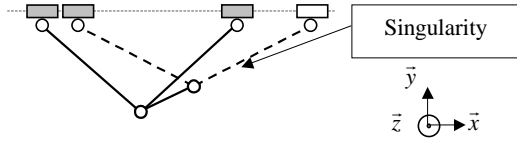


Figure 2. Mechanism singularities.

3. Modeling

3.1. Position equation

Vector $\mathbf{q} = [q_1, q_2, q_3, q_4]^T$ denotes drive positions and $\mathbf{x} = [x, y, \theta]^T$ is the nacelle configuration, described by the position of point C and nacelle orientation (Figure 3).

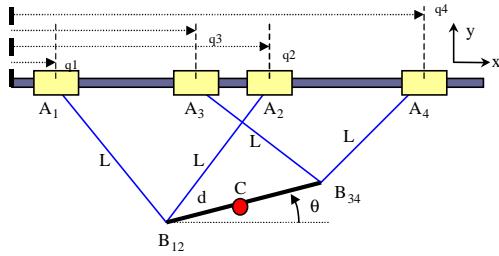


Figure 3. ARCHI parameters.

Coordinates of points \mathbf{B}_{12} (x_{12}, y_{12}) and \mathbf{B}_{34} (x_{34}, y_{34}), are given by:

$$\begin{aligned} x_{12} &= x - d \cdot \cos \theta & x_{34} &= x + d \cdot \cos \theta \\ y_{12} &= y - d \cdot \sin \theta & y_{34} &= y + d \cdot \sin \theta \end{aligned}$$

▪ Inverse position equation

$$q_1 = x_{12} - s_1 \quad q_2 = x_{12} + s_1 \quad q_3 = x_{34} - s_2 \quad q_4 = x_{34} + s_2$$

$$\text{where: } s_1 = \sqrt{L^2 - y_{12}^2}, \quad s_2 = \sqrt{L^2 - y_{34}^2}$$

▪ Forward position equation²

Depending on which set of 3 chains among the 4 is selected, different computations can be made, which are similar to:

$$\begin{aligned} x_{12} &= \frac{1}{2}(q_1 + q_3) & y_{12} &= -\sqrt{L^2 - \frac{1}{4}(q_3 - q_1)^2} \\ x_{34} &= \frac{1}{2}(q_2 + q_4) & y_{34} &= -\sqrt{L^2 - \frac{1}{4}(q_4 - q_2)^2} \end{aligned}$$

The position of point C, and the nacelle angle, are given by:

$$x = \frac{x_{12} + x_{34}}{2}, \quad y = \frac{y_{12} + y_{34}}{2}, \quad \tan(\theta) = \frac{y_{34} - y_{12}}{x_{34} - x_{12}}$$

² For a real machine, results are more accurate with an iterative computation (use of the generalized inverse of the jacobian matrix).

3.2. Velocity equation

As shown in [11], the velocity equation can be written as:

$$\dot{\mathbf{q}} = \mathbf{J}_m \dot{\mathbf{x}}$$

where:

$$\mathbf{J}_m = \begin{bmatrix} 1 & \frac{y_{12}}{s_1} & d \cdot (\sin \theta - \frac{y_{12}}{s_1} \cdot \cos \theta) \\ 1 & -\frac{y_{12}}{s_1} & d \cdot (\sin \theta + \frac{y_{12}}{s_1} \cdot \cos \theta) \\ 1 & \frac{y_{34}}{s_2} & d \cdot (-\sin \theta + \frac{y_{34}}{s_2} \cdot \cos \theta) \\ 1 & -\frac{y_{34}}{s_2} & d \cdot (-\sin \theta - \frac{y_{34}}{s_2} \cdot \cos \theta) \end{bmatrix}$$

3.3. Singularity issue

The Jacobian conditioning index of the redundant machine ARCHI and the Jacobian conditioning index of the 4 non-redundant sub-mechanisms composed of 3 arms ($\text{cond}(\mathbf{J}_{124})$, $\text{cond}(\mathbf{J}_{134})$, $\text{cond}(\mathbf{J}_{123})$, $\text{cond}(\mathbf{J}_{234})$) can be compared to evaluate the contribution of actuator redundancy (Figure 4). The first series of curves depicts the behavior of each set of chains: singularities occur clearly when the condition number tends to infinity. On the contrary, the redundant complete machine offers good conditioning for both matrices, guaranteeing that no singularity occurs (of course, under-mobility singularity still exists for this mechanism, but they are easy to manage as for most parallel mechanisms).

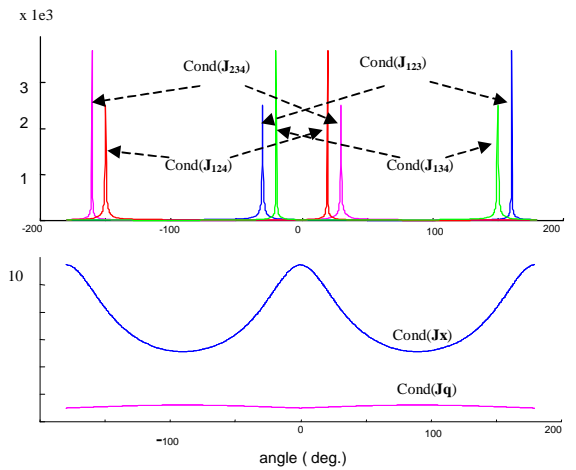


Figure 4. Jacobian conditioning index of redundant and non-redundant mechanisms for $x = 1 \text{ m}$, $y = -0.4 \text{ m}$ and $\theta \in [-180, 180]$ degrees ($L = 1 \text{ m}$, $d = 0.2 \text{ m}$).

3.4. Dynamic equation

Neglecting arms inertia, the following dynamic equation can be derived:

$$[J_m^T M_d J_m + M_n] \ddot{x} + [J_m^T M_d \dot{J}_m + J_m^T K J_m] \dot{x} + f_n + M_n g + J_m^T f_d = 0$$

where:

- f_d and f_n are, respectively, drive and nacelle forces
- M_n is a matrix containing nacelle mass and inertia
- M_d is a matrix containing drive masses
- K is a matrix of drive friction coefficients
- g is a gravity vector.

4. Control strategies simulation results

Using all previous models a simulator of ARCHI including dynamic effects and the possibility of introducing errors on different parameters has been built. Simulation results for a typical motion combining a translation along x and y and a rotation from $\pi/4$ to $\pi/2$ are presented; during that motion, the chain No 4 crosses a singularity.

4.1. Independent joint space control

Most (if not all) industrial machine-tools control systems are based on independent (linear) joint control loops; with actuation redundancy, any dimensional error in kinematic models leads to non-convergence problems as soon as an integral effect is included in the control loops. Figure 5 shows such a problem with a 2% error on one leg length. The idea is then to study an alternate approach (dynamic Cartesian scheme) with different control strategies.

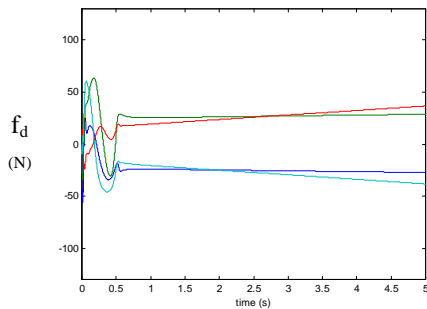


Figure 5. Drive forces do not converge in case of dimensional error.

4.2. General approach: Dynamic Cartesian scheme

To overcome the problems due to dimensional errors, only Cartesian control schemes are proposed; moreover, since parallel mechanisms are intended to offer high speeds and high accelerations, taking into account dynamics seems to be mandatory for better performances (Figure 6).

However, redundancy issue has been considered too: the non-uniqueness of drive forces corresponding to a given external force may be addressed in various ways.

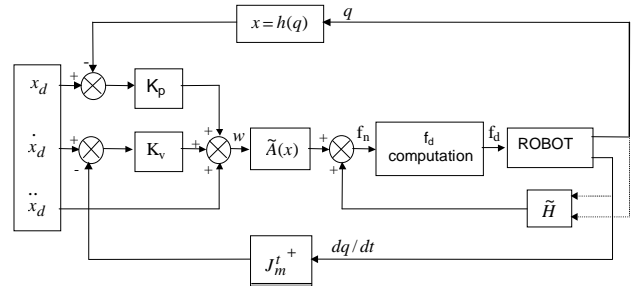


Figure 6. Dynamic Cartesian control structure.

4.3. '2-arm robot like' control

It has been explained in section 2 that ARCHI could be considered as a two-arm robot carrying a solid object. Thus appealing control strategies may be similar to those proposed for two-arm robots; for example, Dauchez *et al.* [13] proposed to define 'internal forces' as forces acting inside the carried object. In a similar way, one can define control strategies where the internal force acting in the nacelle is considered.

4.3.1. Without gravity effect.

The simplest way to consider such 'internal force' is to regard statics only: then the internal force ('inside' the nacelle) is defined as the difference between the static forces, f_1 and f_2 , produced by each 'individual robot' (i.e. each 2-dof sub-part), projected on the nacelle direction (given by vector n in Figure 7). An appealing control strategy is then to set this 'internal force' to zero:

$$(f_1 - f_2) \cdot n = 0$$

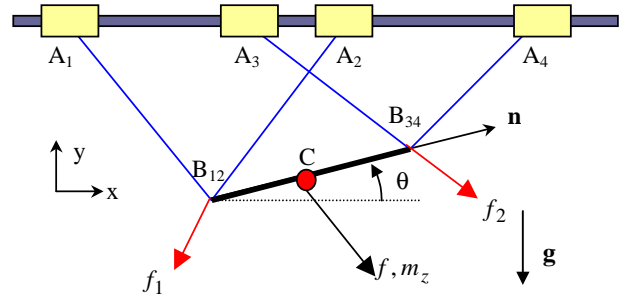


Figure 7. Forces on the mechanism.

This condition leads to:

$$J_f \cdot [f_{1x} \ f_{1y} \ f_{2x} \ f_{2y}]^T = [f_x \ f_y \ m_z \ 0]^T$$

with:

$$\mathbf{J}_f = \begin{bmatrix} 1 & 0 & 1 & 0 \\ 0 & 1 & 0 & 1 \\ d \cdot \sin \theta & -d \cdot \cos \theta & -d \cdot \sin \theta & d \cdot \cos \theta \\ \cos \theta & \sin \theta & -\cos \theta & -\sin \theta \end{bmatrix}$$

Moreover,

$$\mathbf{f}_d = [\mathbf{J}_x^{-1} \cdot \mathbf{J}_q]^T \cdot [f_{1x} \quad f_{1y} \quad f_{2x} \quad f_{2y}]^T$$

Then drive forces are given by:

$$\mathbf{f}_d = [\mathbf{J}_x^{-1} \cdot \mathbf{J}_q]^T \cdot \mathbf{J}_f^{-1} \cdot [f_x \quad f_y \quad m_z \quad 0]^T$$

4.3.2. With gravity effect. In this case, the supplementary condition is:

$$(\mathbf{f}_1 - \mathbf{f}_2) \cdot \mathbf{n} = M_n \cdot g \cdot \sin \theta$$

4.4. Minimizing a given criterion

As $\dim(\text{Ker}(\mathbf{J}_m))=1$, the equation $\mathbf{J}_m^T \cdot \mathbf{f}_d = \mathbf{f}$ has an infinite number of solutions [14][15]:

$$\mathbf{f}_d = \mathbf{J}_m^{T+} \cdot \mathbf{f} + [\mathbf{I} - \mathbf{J}_m^{T+} \mathbf{J}_m^T] \cdot \mathbf{z}, \quad \mathbf{z} \in \mathfrak{R}^4$$

In fact, $[\mathbf{I} - \mathbf{J}_m^{T+} \mathbf{J}_m^T] \cdot \mathbf{z}$ belongs to the null-space [16] and represents internal forces in the mechanism:

$$[\mathbf{I} - \mathbf{J}_m^{T+} \mathbf{J}_m^T] \cdot \mathbf{z} \in \text{Ker}(\mathbf{J}_m)$$

Then, drive forces computation can be realized by minimizing a given criterion [17][18][19] as the 2-norm or the infinite norm of drive forces.

4.4.1. Pseudo-inverse based control. The solution corresponding to $\mathbf{z} = 0$, i.e. the result of a pseudo-inversion, minimizes $\|\mathbf{f}_d\|_2$ (if $\mathbf{z} = 0$, internal forces are equal to zero).

4.4.2. Infinity-norm based control. Minimization of the infinite norm of \mathbf{f}_d can be performed choosing $\mathbf{z} = -k \cdot \text{grad}(\|\mathbf{f}_d\|_\infty)$, $k \in \mathfrak{R}^+$. It corresponds to a minimization of the maximal drive force.

4.5. Simulation results

Following figures (from 8 to 10) give views of actuator forces (4 plots in a figure, corresponding to the four actuators), as well as information about the internal force (1 plot in a second figure, corresponding to the force component that lies in the Jacobian kernel).

Figure 8 describes simulation results in the case of a 2-arm control, where the gravity effects are managed by the control

scheme. Since these effects are not neglected, the static internal force is very small. Note that no divergence occurs (contrary to the case presented in Figure 5). Regarding control using the pseudo-inverse (Figure 9), the result is better than the 2-arm control because drives forces component in the null-space is equal to zero all along the simulated path. Again, no divergence occurs. Figure 10 shows that the minimization of the infinite norm of drive forces is more efficient than the simple pseudo-inverse: actuator forces are kept smaller; however, drive forces present undesirable ‘discontinuities’.

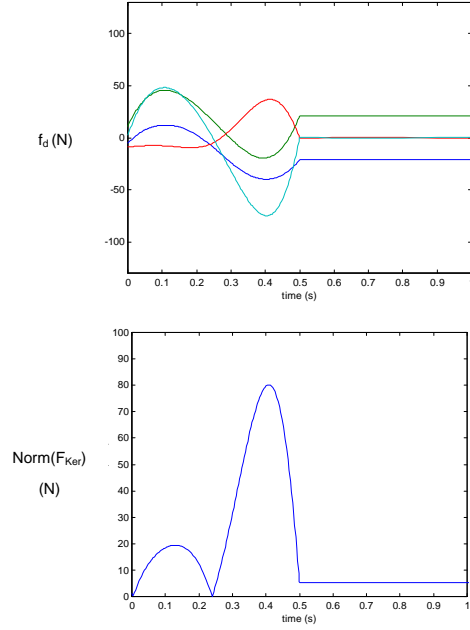


Figure 8. Forces with ‘two-arm like’ control, with gravity.

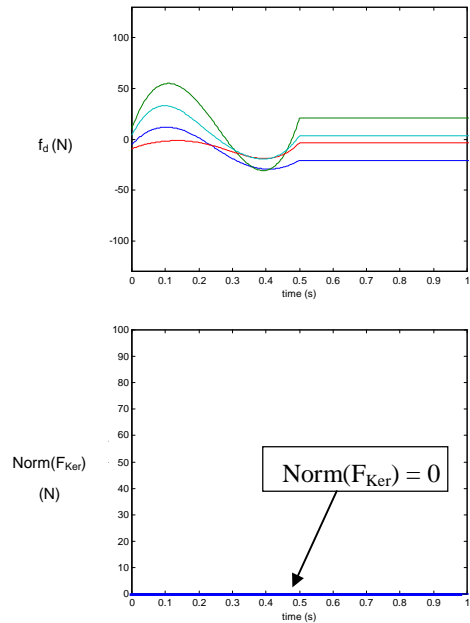


Figure 9. Pseudo-inverse based control.

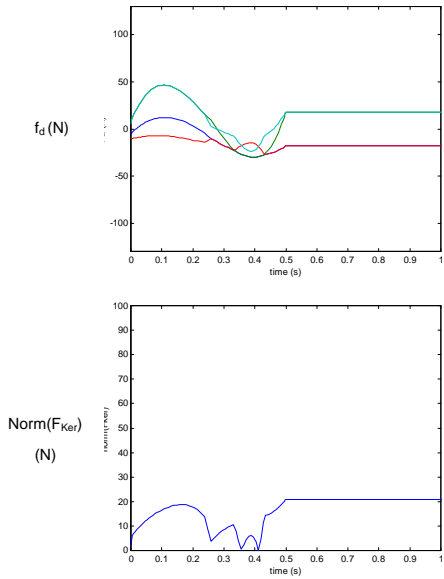


Figure 10. Infinity-norm based control.

5. First experimental results

Figure 11 presents our first prototype. The complete control system is implemented on a single PC (Pentium II, 200 MHz, 64 Mb) running Windows NT4, without any control board; indeed, a lab-made I/O board is plugged into the PCI bus and connects the PC to the amplifiers by means of analog signals, and the position encoders to the PC by means of digital signals. This means that both the Graphical User Interface (G.U.I.) and the Position Control are running on the same PC; this relies on the use of RTX, a software package that enables Real-Time processes to run on a PC while keeping advantages of Windows NT environment.

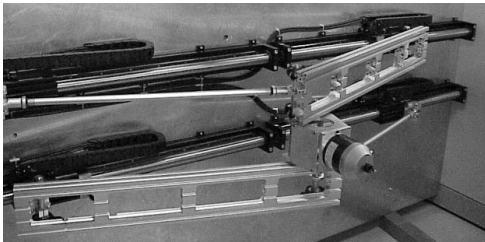


Figure 11. A picture of the first ARCHI prototype ($L=1\text{ m}$, $d=0.055\text{ m}$).

- **Windows-NT process.** It is a G.U.I. where displacement parameters (desired position, maximal velocity, etc) and control parameters can be set. User can query data as well.
- **Real-time process.** Real-time process main tasks are to generate a trajectory and to control the position. Trajectory generation is realized in Cartesian Space, according to a 5th order polynomial in position insuring accelerations continuity (even if it doesn't optimize displacements). The control task is defined as a periodical task with maximal priority, and runs at a 2kHz frequency.

The control scheme was described in Figure 6, however the inverse dynamic model is not implemented yet and forces computation is realized by using the generalized inverse of the jacobian matrix (Figure 12).

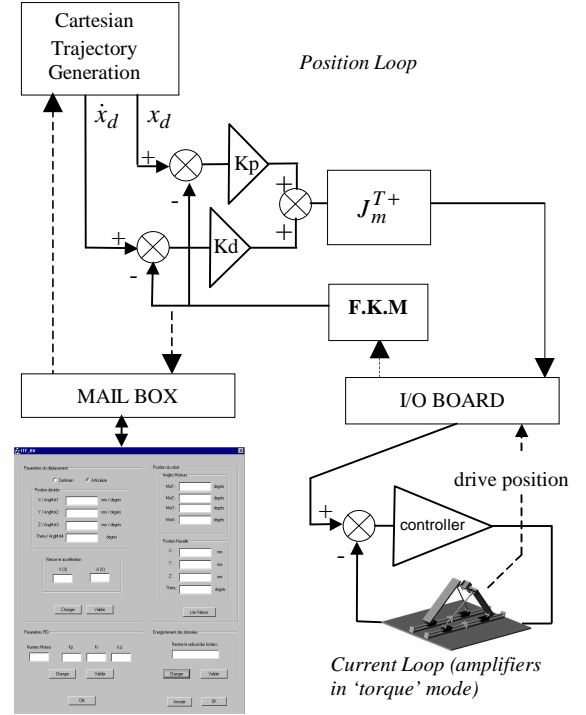


Figure 12. Control implementation.

The results presented below (Figures 13 to 16) have been obtained for displacements from positions $x_i = [1.1, -0.6, \pi/2]^T$ to $x_f = [1.15, -0.65, -\pi/2]^T$ (forward and backward displacements) crossing singular positions of non-redundant subsystems.

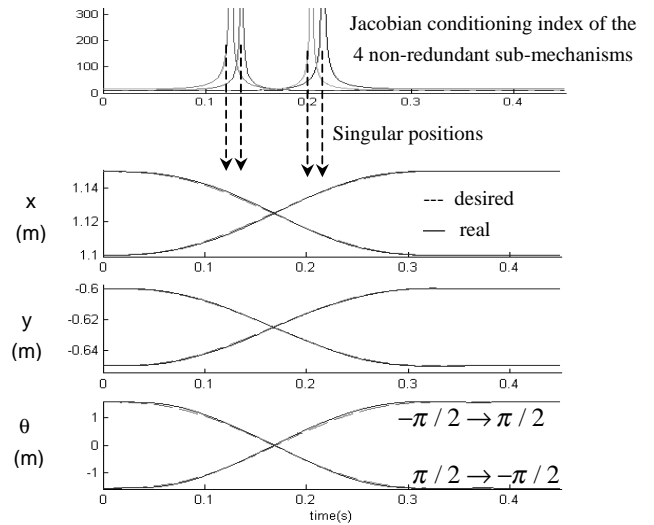


Figure 13. Nacelle position during a displacement crossing singular positions.

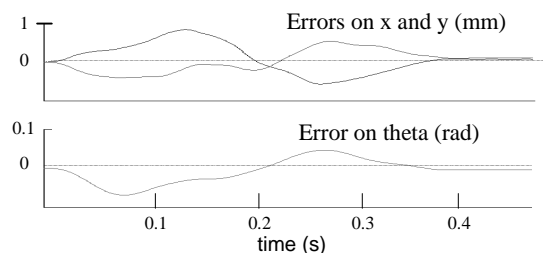


Figure 14. Errors on x , y and θ during the displacement.

Figure 15 represents actuator forces (f_d) during the displacement described above.

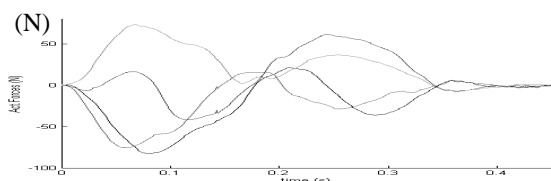


Figure 15. Actuator forces.

A projection on the null-space (kernel) associated to the Jacobian matrix permits to compute internal forces on the mechanism (Figure 16). These internal forces keep small compared to drive forces (theoretically they are equal to zero) and forces computation based on the using of generalized inverse seems to be simple and efficient.

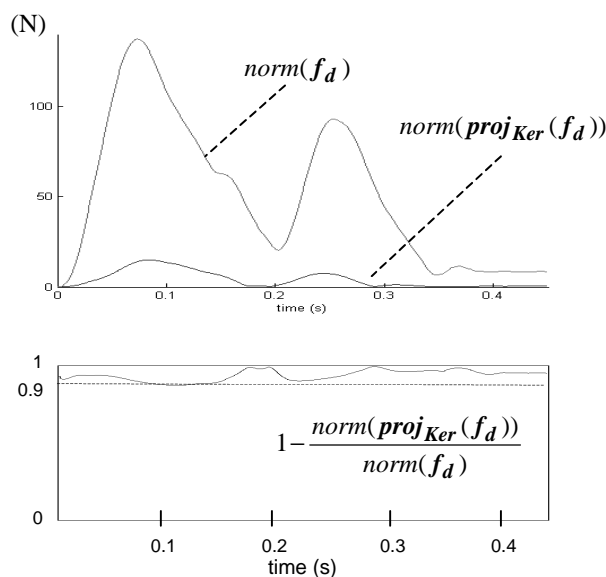


Figure 16. Internal forces on the mechanism.

6. Conclusion

In this paper ARCHI, a new 3-dof redundant parallel robot actuated by four drives, has been described. Its kinematic and dynamic models were given; its ability to easily evolve in the whole workspace and to allow unlimited rotations has been proven. Simulations based upon different joint forces computations methods were compared. A prototype has

been built and the implementation of a first set of control procedures has been carried out. Preliminary tests demonstrate it is actually possible to use redundancy to overcome over-mobility singularities in a machine dedicated to high speed motions.

Future tests will offer a concluding view about which control strategy fits properly our need.

Then, ARCHI robot will be included as a part of an hybrid robot dedicated to machining.

7. References

- [1] Gough V.E., Contribution to discussion of papers on research in automotive stability, control and tyre performance. Proc. Auto Div. Inst. Mechanical Engineers, 1956-1957.
- [2] Stewart D., A platform with 6 degrees of freedom. Proc. of the Inst. of Mech. engineers, 180 (Part 1, 15), pp. 371-386, 1965.
- [3] Merlet J.-P., Les robots parallèles, 2nd Edition, Hermes, 1997.
- [4] Tönshoff H.K., A systematic comparison of parallel kinematics. Keynote in Proceedings of the First Forum on Parallel Kinematic Machines, Milan, Italy, August 31- September 1, 1998.
- [5] Clavel R., Une nouvelle structure de manipulateur parallèle pour la robotique légère, APII, 23(6), pp. 501-519, 1989.
- [6] Pierrot F., Dauchez P. and Fournier A., Fast parallel robots. Journal of Robotic Systems, 8(6), pp. 829-840, 1991.
- [7] Pierrot F., Shibukawa T., From Hexa to HexaM. In Proc. IPK'98: Internationales Parallelkinematik-Kolloquium, Zürich, June 4, pp. 75-84, 1998.
- [8] Siciliano B. The Tricept robot: inverse kinematics, manipulability analysis and closed-loop direct kinematics algorithm. Robotica, 17:437-445, 1999.
- [9] Kim J. and Park F.C., Eclipse – A new parallel mechanism prototype. Position paper in Proceedings of the First European-American Forum on Parallel Kinematic Machines, Milan, Italy, August 31- September 1, 1998.
- [10] Pierrot F., Marquet F., Company O., Gil T., H4 parallel robot: modeling, design and preliminary experiments. IEEE Int. Conf. On Robotics and Automation, Seoul, Korea, May 2001.
- [11] Innocenti C. and Parenti-Castelli V., Exhaustive enumeration of fully parallel kinematic chains. Dynamic System and Control, Vol. 55-2, pp. 1135-1141.
- [12] Marquet F., Krut. S., Company O., Pierrot, F., Archi, a redundant mechanism for machining with unlimited rotation capacities, to appear in Proc. of ICAR 2001, Budapest, August 2001.
- [13] Dauchez P., Delebarre X., Jourdan R., Hybrid control of a two-arm robot handling firmly a single rigid object, Proc. of the 2nd SIFIR, Saragoza, Spain, pp. 67-72, November 1989.
- [14] Kock S., Schumacher W., A mixed elastic and rigid body dynamic model of an actuation redundant parallel robot with high-reduction gears, IEEE Int. Conf. On Robotics and Automation, April 2000.
- [15] Dasgupta B., Mruthyunjaya T.S. Force redundancy in parallel manipulators: theoretical and practical issues. Mechanism and Machine Theory, 33(6):pp. 727-742, August 1998.
- [16] Kock S., Schumacher W., A parallel x-y manipulator with actuation redundancy for high-speed and active stiffness applications. IEEE Int. Conf. On Robotics and Automation, Leuven, Belgium. Vol. 3: pp. 2295-2300, May 1998.
- [17] Kurtz R., Hayward V., Multiple goal kinematic optimization of a parallel spherical mechanism with actuator redundancy, IEEE Int. Conf. On Robotics and Automation, Vol. 8, N° 5. pp. 644-651. October 1992.
- [18] Yoshikawa T., Analysis and control of robot manipulators with redundancy, The int. Journal of Robotics research, Vol. 4, 1985.
- [19] Kokkinis T. et Millies P., A parallel robot-arm regional structure with actuation redundancy. Mechanism and Machine Theory, 26(6): pp. 629-641, 1991.

Acknowledgements: This work has been partially supported by the European Commission, GROWTH Program, GIRD CT1999 00150.